Proc. Indian Acad. Sci. (Earth Planet. Sci.), Vol. 93, No. 4, November 1984, pp. 399–411.

Seasonal variability of the temperature field off the south-west coast of India

SATISH R SHETYE

Physical Oceanography Division, National Institute of Oceanography, Dona Paula, Goa 403 004, India

MS received 4 February 1984; revised 20 July 84

Abstract. The temperature field in the coastal region off south-west India exhibits a well-marked annual cycle. Around March the isotherms develop an upward tilt near the coast. The magnitude of the tilt increases continuously till August, then decreases and vanishes in November. To check the hypothesis that this feature is in response to the local wind, we have used the resultant wind data to determine the annual march of the wind stress. It is found that though weak during November–March, the monthly-mean longshore component of the wind stress is always conducive to coastal upwelling and follows a pattern similar to that of the isotherm tilt. We interpret this result to indicate that coastal processes in the area during April–October are controlled by the longshore component of the local wind stress in accordance with the classical model for a coastal upwelling system. During November–March, when the wind stress is weak, it appears that the influence of the longshore density gradient, which persists at the surface during this period, dominates over the effect of the wind.

Keywords. Temperature field; Indian coastal region; wind stress; coastal upwelling; Ekman-Thorade model; wind-forcing; thermohaline forcing; advective field.

1. Introduction

The region of interest for this study stretches from 8° N to about 15° N along the south-west coast of India. As shown in figure 1, the coast lies along almost a straight line at an angle of about 24° with the north. Off the coast the bottom topography consists of a continental shelf which is about 60 km wide, a continental slope where the depth increases from 200 m to 2000 m, followed by a region of uniform depth of approximately 2000 m.

Most of the information on the physical oceanography of this region is derived from the hydrographic surveys conducted during the last couple of decades. These surveys have documented the seasonal variability in the salinity and temperature distribution in the area. One feature that has been demonstrated by these studies is that all along the coast, the deeper, colder water is generally found at shallower depths during June–July–August than during December–January–February (see; for example, Sharma 1968; UNDP/FAO Report 1976).

What causes this seasonal shallowing of the isotherms close to the coast? Two explanations have so far been mooted. The first, which for convenience may be labelled 'remote forcing hypothesis', assumes that the currents off the south-west coast are forced by the wind- and thermohaline-forcing over the whole of the Arabian Sea; local forcing is assumed negligible. In this scenario the shallowing of the isotherms near the coast is considered a manifestation of a remotely forced southward geostrophic coastal current. The second explanation, 'local forcing hypothesis', invokes the classical

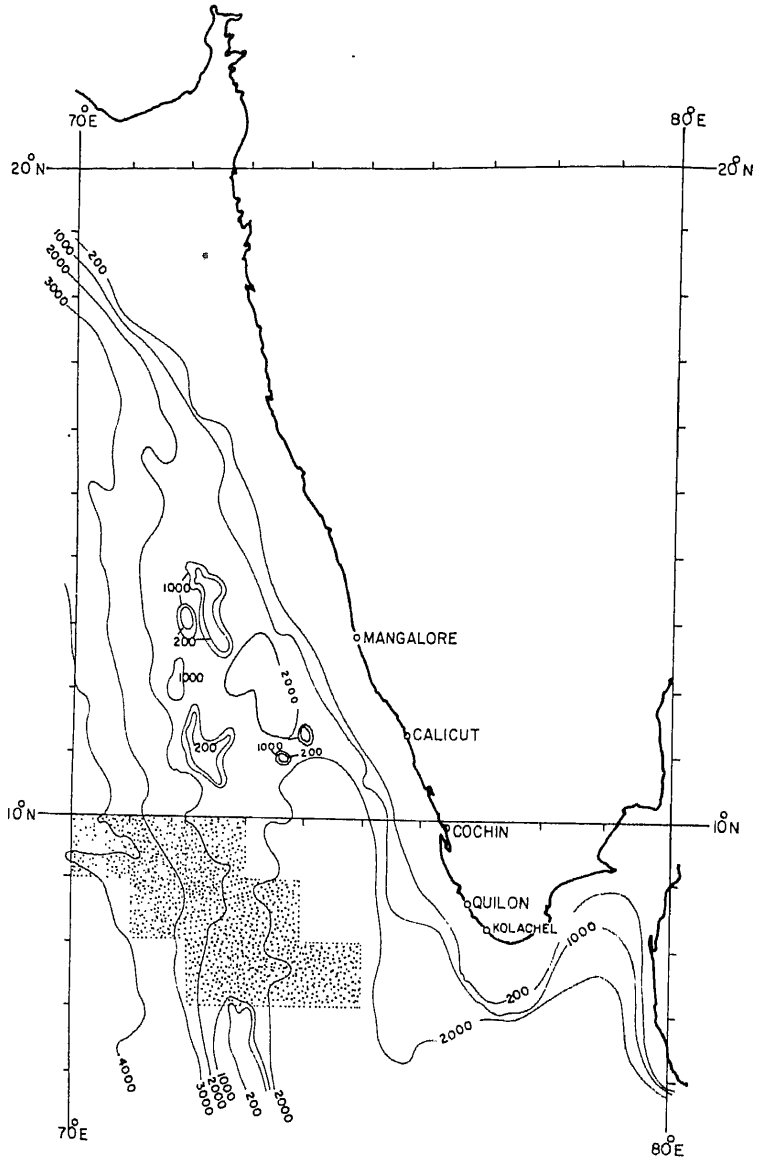

Figure 1. The area of interest lies roughly between the southern tip of India and the 15°N latitude. Monthly mean winds for the dotted region have been used in §3. The bottom topography contours are in metres.

Ekman-Thorade model (Sverdrup *et al* 1942) of coastal upwelling. Here the shallowing of the isotherms is attributed to an ascent of water near the coast, due to a compensatory replacement of surface water when an offshore transport of surface water has resulted from a more or less northerly wind blowing parallel to the coastline.

The validity of the two mechanisms stated above needs to be scrutinised to understand even the gross features of the coastal processes in the region. The purpose of the present note is to examine the 'local forcing hypothesis' in a little greater detail than

was done in earlier studies. In §2 the salient features of the month-to-month variability of the thermal structure in the region are described and the meagre existing estimates of the advective field are outlined. §3 examines the local forcing functions and their implications in the thermal and the advective field. The conclusions are summarized in §4.

2. The seasonal variability in the temperature field

Before examining the behaviour of the thermal structure in the coastal region, it is instructive to identify the features of the vertical variation in temperature away from the coast. A typical vertical temperature profile in the Central Arabian Sea (Wyrtki 1971) shows: (a) The mixed layer: Its depth may lie anywhere from 40 to 100 m and the behaviour of this turbulent layer is controlled mainly by the exchange of momentum and buoyancy across the air-sea interface, (b) The upper thermocline: This layer is characterized by a large temperature gradient and the 20°C isotherm is usually located in the middle of this layer, which occupies the region roughly between the depths of 70 and 300 m though some seasonal variation has been noted, (c) The lower thermocline: This is a continuation of the upper thermocline, but the temperature gradient is weaker, its depth is arbitrarily fixed from 300 to 1000 m, (d) The deep layer: This is a layer of relatively slow change in temperature and stretches from 1000 m to the bottom.

Closer to the coast, within about 250 km from the coastline, the thermal structure outlined above is modified due to processes peculiar to the coastal region. Restricting attention to a time scale of a month or longer, the principal feature of this change is represented in figure 2. Taken from the UNDP/FAO Report (1973), the figure shows temperature sections more or less normal to the coast off Cochin. The horizontal distance covered by each section is approximately 100 km. The December section (figure 2C) shows a mixed layer in which the temperature is a little over 28°C, and has a depth of around 30 m. The 20°C isotherm, which lies in the middle of the upper thermocline, occurs at a depth of approximately 120 m. Note that this isotherm is horizontal. This is in contrast to the thermal structure in figure 2A. This section, made in the month of July, also off Cochin, shows a marked tilt to all isotherms. The shallowing of the isolines, on approaching the coast, is not confined to the temperature field alone. It is also noticeable in the oxygen distribution, as seen from figures 2B and 2D.

The nature of the tilt in the isotherms is also brought out by the maps of 20°C isotherm topography given in the Atlas of the International Indian Ocean Expedition (Wyrtki 1971). Figure 3, based on these maps, shows the isotherm topography for the months of January–February (3A), and that for July–August (3B). A comparison between the two figures indicates that the shallowing is confined to a strip, less than 300 km wide, all along the coast. During January–February, the depth of the 20°C isotherm very near the coast, is virtually the same ($\approx$ 120 m) as that far away from it. In July–August, however, the same isotherm close to the coast lies at a depth of less than 60 m, while farther offshore the depth continues to be around 120 m.

How does the depth of the 20°C isotherm along the coast vary from month-to-month? Sharma (1968) using temperature sections similar to those given in figure 2 has constructed plots that give month-to-month variation in mean temperature at a given depth on the shelf. By horizontally integrating a section, Sharma determines the mean

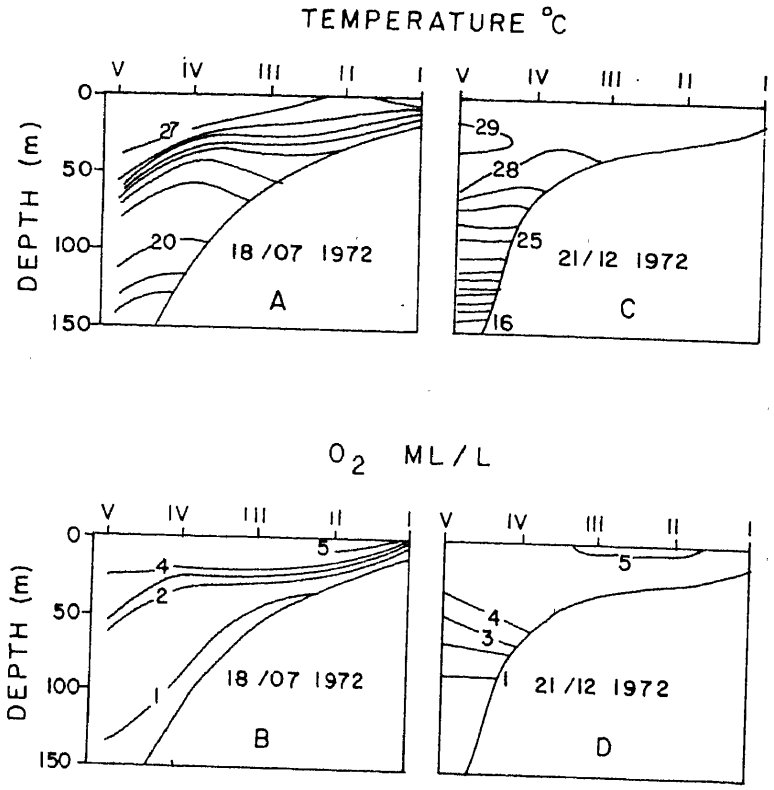

Figure 2. Temperature and oxygen sections off Cochin. Horizontal distance covered by each section is about 100 km. Data in A and B were recorded on 18th July 1972; C and D on 21 December 1972.

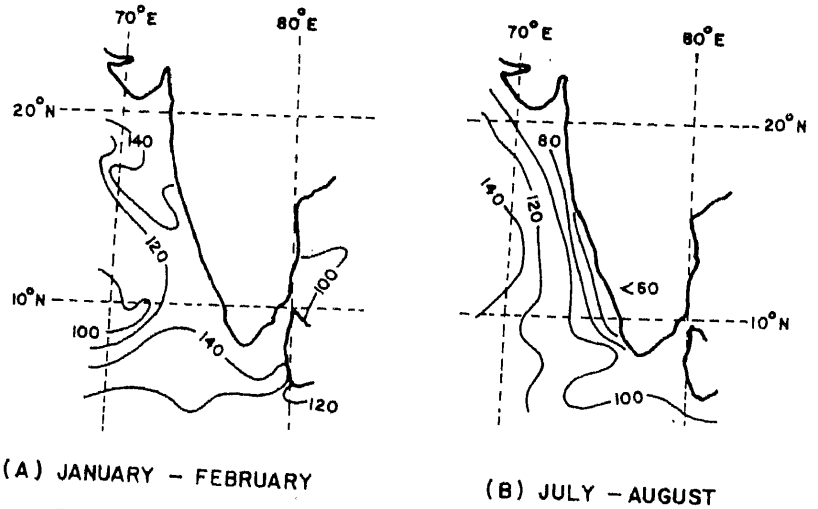

Figure 3. Depth of the 20°C isotherm. (A) January–February; (B) July–August.

temperature at different depths. Similar profiles for different months are then assembled to construct isotherm contours on a graph with depth and month as the two axes. Figure 4 reproduces Sharma's 20°C isotherm contours at various locations along the coast. At Cochin similar plots for a part of 1971, and the whole of 1972 and 1973 are available from the UNDP/FAO Report (1974). In spite of both spatial and interannual variability, figure 4 shows a well-marked annual cycle. In figure 5, all the curves from figure 4 are assembled to construct an envelope (light lines) to the 20°C contours. The mean contour for the envelope is shown by a solid line. From figures 2–5 it becomes apparent that the near coast shallowing of the isotherms begins in March; by August the isotherms are located at the shallowest depth. From late August to November, the tilt in the isotherms decreases and vanishes by November. The depth of the isotherms remains relatively unchanged during December–January–February.

Theoretical considerations as well as observations suggest that in coastal systems the thermohaline field and the advective field act in unison; *i.e.* a change in the thermohaline field is accompanied by a corresponding change in the advective field. A similar behaviour might be expected off the south-west coast. Unfortunately, data on the advective field off this coast are very few. The only information available at present on the month-to-month evolution of coastal currents comes from ship-drift estimates (KNMI 1952, Atlas of The Surface Currents—Indian Ocean 1970). These data provide clues on the advective field near the ocean surface. Direct observations of currents deeper in the water column for a time interval long enough to identify its monthly mean have not yet been made. Available ship-drift measurements generally show longshore surface currents off the coast set towards the south from March to September. The current is strongest in July–August with a mean velocity of the order of 30 cm/sec. A weak current towards the north persists between November and January. The northward current is strongest in December, its longshore component being 15 cm/sec approximately. October and February are transition months. It is not clear whether or not the flow deeper in the water column exhibits a behaviour similar to that at the surface. In literature it is often tacitly implied that it does. However, this is yet to be established.

3. Local forcing functions and their implications in the thermal and the advective field

Consider a north-south coast with a sea to the west of it. Let the local wind field be such that the longshore component points towards the equator, and the cross-shore towards the east. In such a situation, according to the well-known coastal upwelling models (Sverdrup *et al* 1942), the response of the coastal waters will be as follows. In the upper Ekman layer the longshore wind will force the water away from the coast. This produces a drop in the sea surface near the coast, and more importantly, waters below the Ekman layer upwell to compensate for the offshore Ekman transport. Due to the upwelling, the isopycnals close to the coast tilt upward, and an equatorward current sets in. The current, with maximum velocity at the surface, is tied to the upwelling-induced slope of the isopycnals near the coast. The longshore component of the wind stress controls both the magnitude of the tilt and the strength of the current. The resulting situation is represented schematically in figure 6. A detailed analysis of this problem can be found in Allen (1973) and in Pedlosky (1974) among other references. These studies also predict that the circulation of the type described above occurs

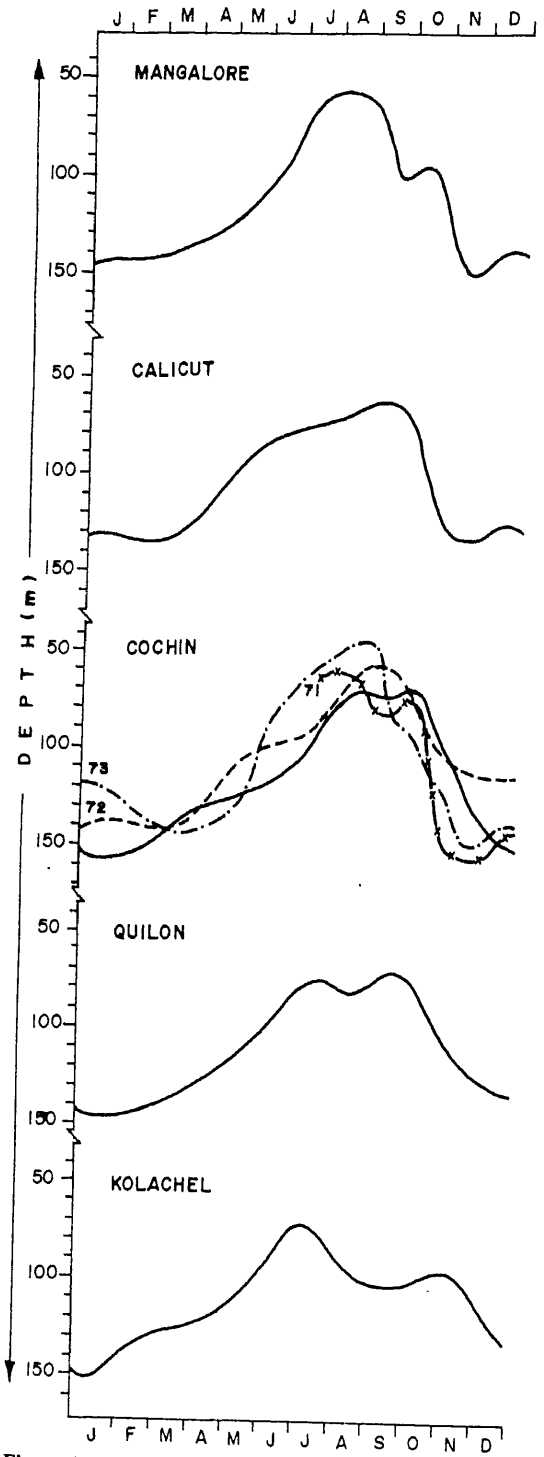

Figure 4. Month-to-month variation in the 20°C contour. The method used in drawing the contour is described in §2. All the solid curves are taken from Sharma (1968); curves marked 71, 72 and 73 for Cochin are taken from the UNDP/FAO Report (1974).

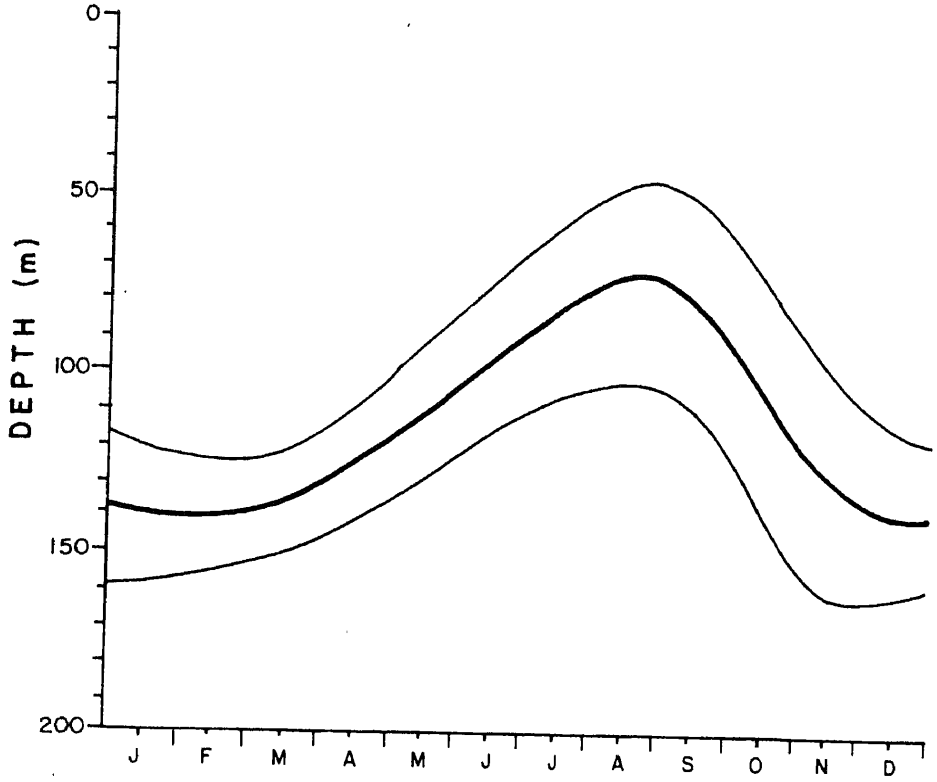

Figure 5. Envelope (light lines) and the mean (solid line) of the contours shown in figure 4.

approximately over a distance of an internal Rossby radius of deformation from the coast. The radius of deformation for the south-west coast is of the order of 200 km. In the region of the coastal jet both advection and diffusion of heat are considered significant in maintaining a thermal equilibrium.

Besides the wind, coastal currents can also be forced by a longshore density gradient imposed at the surface (thermohaline-driving). In the northern hemisphere, if the surface density increases (decreases) towards the north the resulting current is northward (southward). A comparison between the magnitudes of the wind-driven component versus the thermohaline-driven component of the current at the surface can be made by comparing

$$F_w = \tfrac{1}{2}\tau_l \qquad \text{with} \qquad F_t = \frac{g}{3}H^2\Delta.$$

Here F_w represents the wind-driven contribution and F_t the thermohaline-driven contribution (see equation 10.1 of Pedlosky 1974). τ_l, g, H and Δ are longshore wind stress, acceleration due to gravity, mean depth of the shelf, and longshore surface density gradient, respectively.

Figure 7 shows the monthly mean winds in the region of interest. The arrows and the isolines of the resultant wind on a (1° × 1°) grid are taken from Hastenrath and Lamb (1979). In figure 1 an area of nine (1° × 1°) squares has been marked with dots. For this area monthly mean wind, based on ship observations, is available in the US Navy

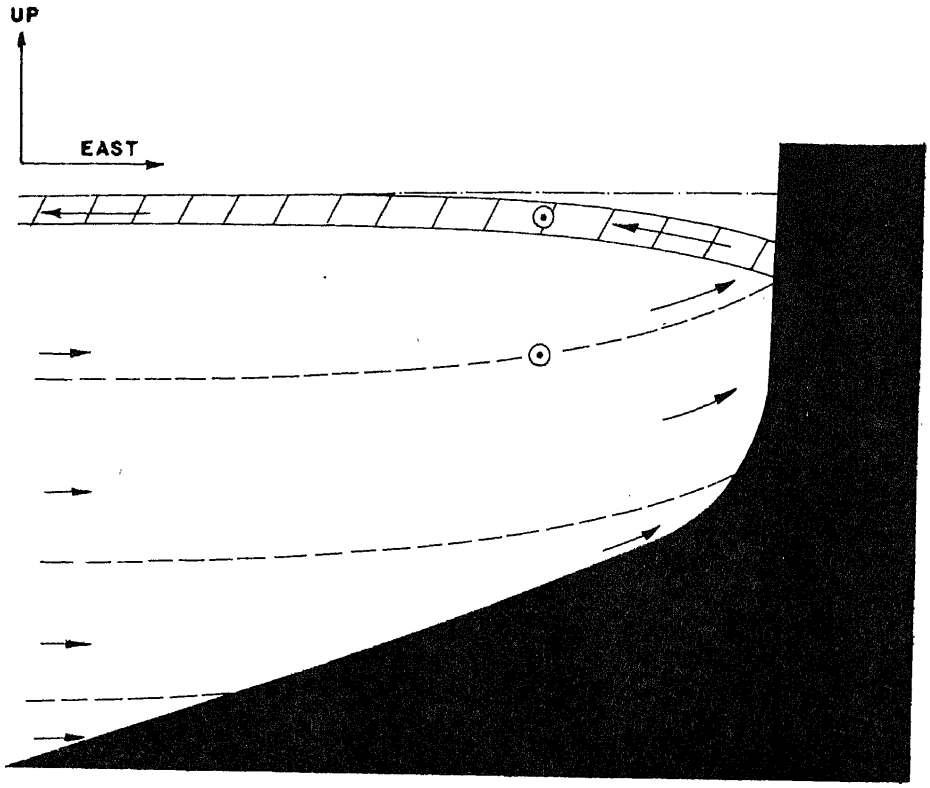

Figure 6. Schematic representation of the effect of wind on coastal processes for a north-south coastline. The longshore component of the wind stress assumed in the figure is towards the equator (*i.e.* coming out of the plane of the paper); the cross-shore component is toward the coast. The surface Ekman layer is shown hatched; in this layer the longshore flow is towards the equator, cross-shore away from the coastline. Below the Ekman layer the longshore current is towards the equator; the cross-shore towards the coast. The sea level in the absence of wind stress is shown by (—— · ——). The dashed lines are isopycnals.

Marine Climatic Atlas (1976). These data are also shown in figure 7. Note that the two data sets are mutually compatible. The figure brings out an interesting feature: monthly-mean wind along the south-west coast always blows in a direction such that the longshore component points towards the equator. This feature of the winds is consistent with other data sources as well. KNMI Atlas (1952) shows behaviour identical to that in figure 7. And, the overall pattern exhibited by MONEX 850 mb winds (Krishnamurti *et al* 1979, 1980a, b) during May–July 1979 is similar to that seen in figure 7 for the period May–July.

The above behaviour of the resultant winds implies that the longshore component of the wind stress is always conducive to upwelling. This is brought out in figure 8 in which the longshore and the offshore components of the stress are plotted. To compute the stress the data from the US Navy Marine Climatic Atlas (1976) are used in the bulk aerodynamic formula

$$\tau = \rho_{air} C_D \mathbf{U} U,$$

where τ is the wind stress vector, $\mathbf{U}$ is the resultant wind vector with magnitude U, ρ_{air} is

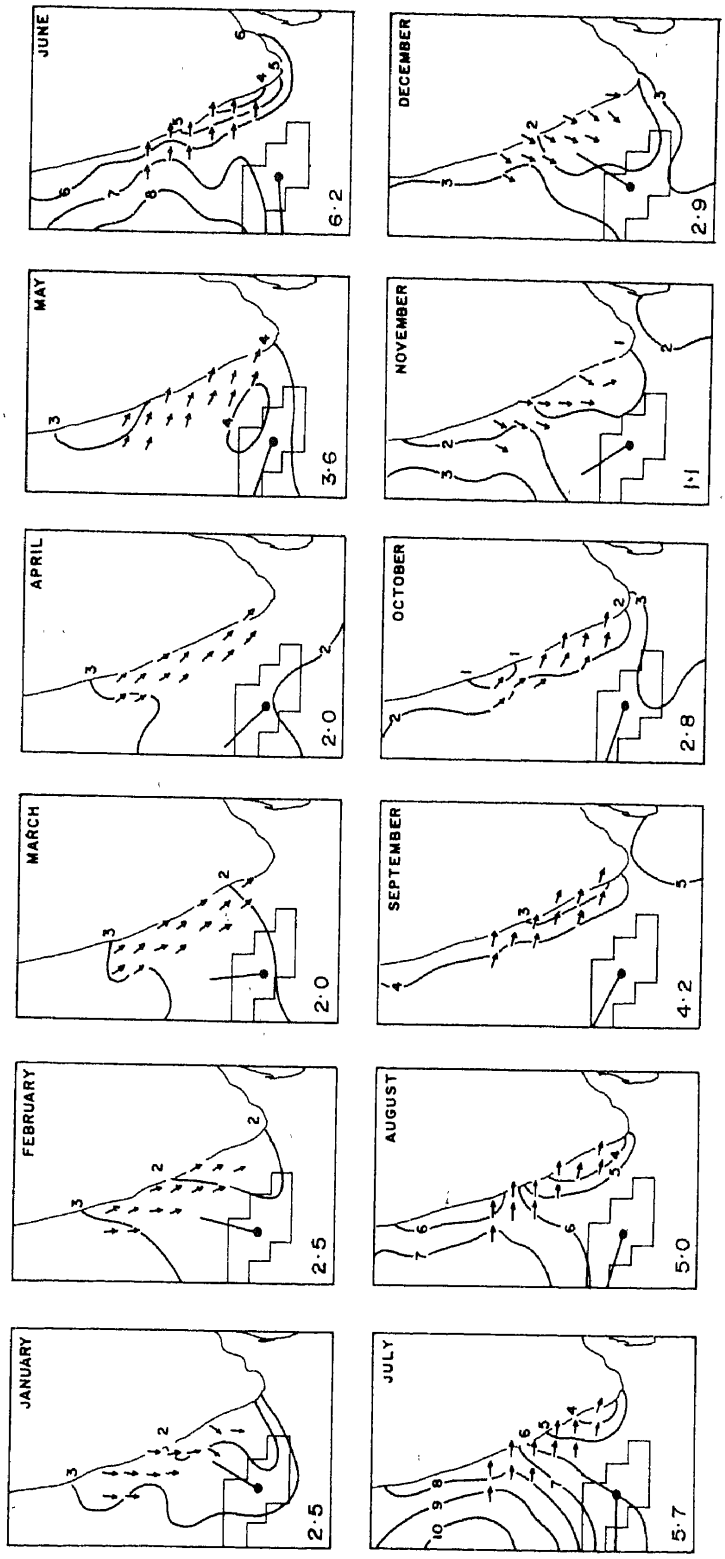

Figure 7. Monthly mean winds in the region of interest. The arrows showing the direction, and the isolines showing the magnitude in m/s, are taken from Hastenrath and Lamb (1979). Monthly mean wind for the area shown dotted in figure 1 is given by a stick, the wind direction being towards the dot at the centre; magnitude (m/s) is shown in the lower left hand corner.

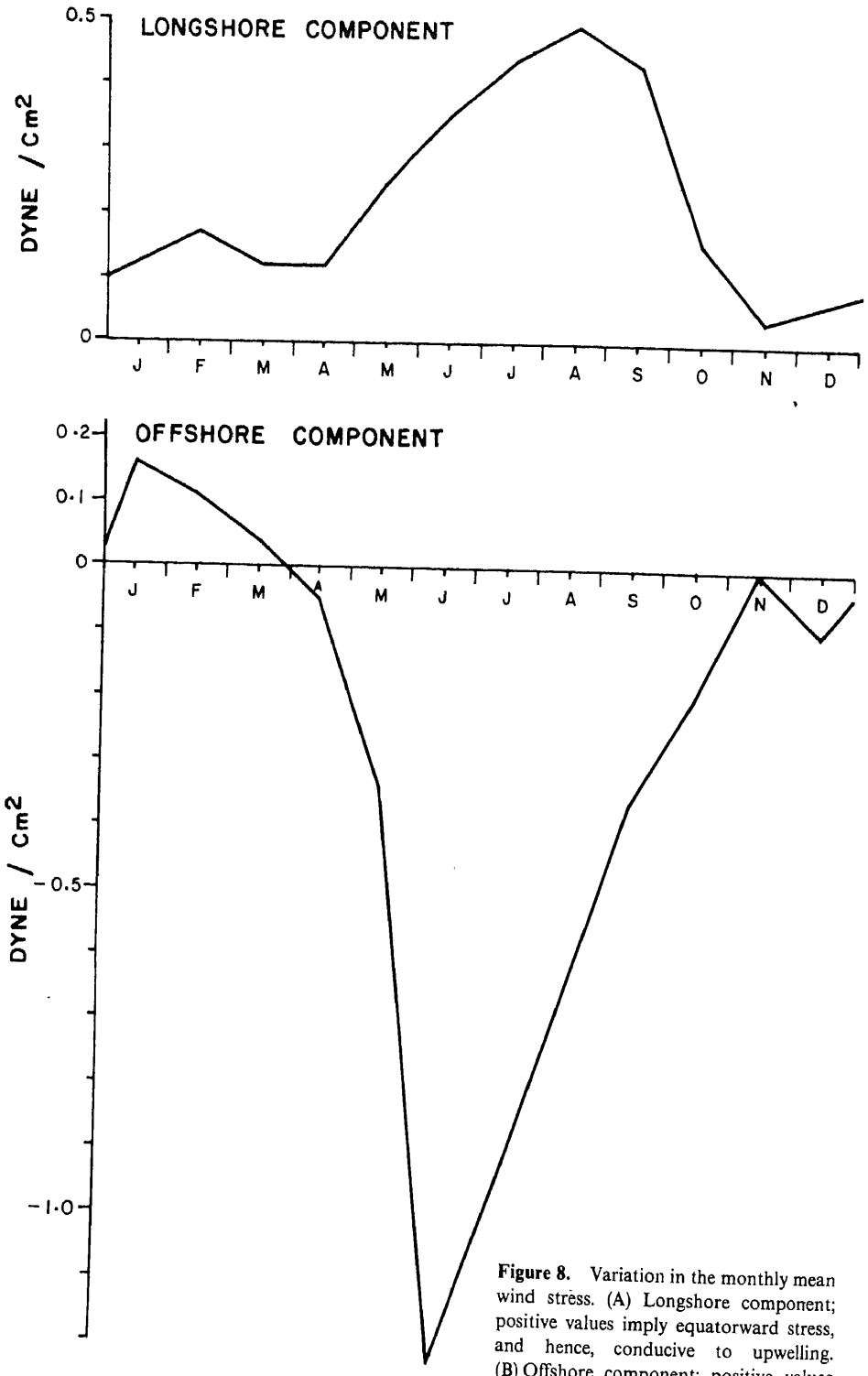

Figure 8. Variation in the monthly mean wind stress. (A) Longshore component; positive values imply equatorward stress, and hence, conducive to upwelling. (B) Offshore component; positive values imply stress away from the coastline.

the density of air and C_D is the drag coefficient. To be consistent with Hastenrath and Lamb (1979) a value of $2{\cdot}8 \times 10^{-3}$ was assigned to C_D, even though this is much larger than the generally used value of 1·3. The offshore (τ_0) and the longshore (τ_l) components were determined by decomposing τ in an orthogonal frame with the normal (pointing away from the coast), and the tangent (pointing towards the equator) to the coast as the two axes respectively. The coastline was approximated by a straight line making an angle of 24° with the north. In this frame a positive (negative) longshore component implies a condition conducive to upwelling (downwelling), and a coastal current towards the equator (pole).

Figure 8 shows that τ_l in the area of interest is weak from November to February, gradually increases from April to August when it reaches a maximum, and then decreases. The decrease occurs faster than the increase. If the monthly mean processes in this coastal region are controlled by the local wind driving in accordance with the model described earlier, it might be expected that the tilt of the isotherms near the coast will also follow a pattern similar to that of τ_l. It is gratifying to note that figures 5 and 8A bear this out. The depth of the 20°C isotherm decreases gradually from April to August, when the isotherm lies at its shallowest depth, then increases rapidly. Between November and March the depth of the isotherm shows little change. If at all a change in the depth of the isotherm occurs during this period, it is much too small to be discernible by the hydrographic data used in the present study.

It was pointed out earlier that the surface current off the south-west coast is set towards the equator approximately between March and September; this current reaches a peak in July–August. Hence, both the magnitude of the upward tilt of the 20°C isotherm, and the strength of the equatorward current in the area of interest follows a pattern similar to that of τ_l during the period approximately from February to October. This result encourages us to conclude that during this period the monthly mean processes are predominantly wind driven according to the classical theory of coastal upwelling.

During November to April, when τ_l is weak and no marked shallowing/deepening of the isotherms is noticed near the coast, a surface current flows towards the north. As τ_l points towards the south during this period, it could not generate this current. Therefore, it is necessary to look at an alternative driving mechanism, such as the thermohaline-driving. The surface density along the south-west coast is generally higher towards the north. Hence, the thermohaline-driven component of the longshore current will tend to induce a northward flow. Magnitude of the surface density gradient changes considerably from season to season. According to the IIOE Atlas (Wyrtki 1971) the mean surface density gradient along the south-west coast between May and October is virtually zero; the same for November–April is $1{\cdot}9 \times 10^{-11}$ g/cm^4. The relative importance of the thermohaline- and the wind-forcing as a generator of the surface current can be compared by determining F_w and F_t defined earlier. During August, F_w, representing the wind-forcing is 0·25 dyne/cm^2, whereas F_t (thermohaline-forcing) is negligibly small. During November to April F_w is on an average 0·05 dyne/cm^2; F_t on the other hand is 0·6 dyne/cm^2. In the latter the mean shelf depth has been taken to be 100 m. These considerations suggest that the northward flowing surface current during November–January arises mainly due to the longshore surface density gradient that persists along the coast during this period. The behaviour of the current during the tail end of this period would be decided by the strength of the surface density gradient versus the strength of the longshore wind stress component.

3. Conclusions

The present study was undertaken as a preliminary examination of the proposition that the seasonal variability of the coastal processes off the south-west coast of India is controlled by the local forcing alone. In view of the discussion in the previous sections we are encouraged to conclude:

(a) During April–October, the coastal processes are generally controlled by the local wind stress. The behaviour of the isotherms, and the nature of the surface current during this period is consistent with the classical model of a typical coastal upwelling system (Sverdrup *et al* 1942).

(b) During November–January, the wind driving is weak and the coastal processes are dominated by the local surface longshore density gradient. The northward flowing coastal surface current at this time is a response to this gradient.

A precautionary note to the above conclusions is in order. The data-base on which these conclusions rest leaves a lot to be desired. Observations are needed to examine in detail the implications of the models considered here. Specifically, it would be helpful to make direct current measurements at a few vertical locations in the water column for a period long enough to identify the seasonal signal, and to examine its relationship to the local forcing functions. Such a set of observations would also help identify the nature of the vertical variability of the current field. Observations in coastal upwelling ecosystems often show the presence of a deep current flowing in a direction opposite to that at the surface. It is possible that such an undercurrent exists off the south-west coast of India. Observations suggested above would help to check this interesting possibility.

Acknowledgements

During the course of this study the author was supported by a Research Associateship in the Physical Oceanography Division of the National Institute of Oceanography. Thanks are due to Dr V V R Varadachari for his interest, and to Dr J S Sastry for his suggestions and comments.

References

Allen J 1973 *J. Phys. Oceanogr.* **3** 245

Atlas of the surface currents—Indian Ocean 1970 (Washington D.C.: United States Navy Hydrographic Office)

Hastenrath S and Lamb P 1979 Climatic Atlas of the Indian Ocean Part 1: Surface Climate and Atmospheric Circulation (Madison: The University of Wisconsin Press)

KNMI (Koninklik Netherlands Meteorolgisch Institunt) 1952 Indische Ocean Oceanograpische en Meteorologische Gegevens 2 Ed. Publication 135

Krishnamurti T N, Ardanuy P, Ramanathan Y and Pasch R 1979 Quick Look "Summer MONEX Atlas" Part 2—The onset phase, Florida State University Report No. 79–5

Krishnamurti T N, Greiman P, Ramanathan Y, Pasch R and Ardanuy P 1980a Quick Look 'Summer MONEX Atlas' Part 1—Saudi Arabia Phase, Florida State University Report No. 80–4

Krishnamurti T N, Ramanathan Y, Ardanuy P, Pasch R and Greiman P 1980b Quick Look 'Summer MONEX Atlas' Part 3—Monsoon Depression Phase, Florida State University Report No. 80–8

Pedlosky J 1974 *J. Phys. Oceanogr.* **4** 214

Sharma G S 1968 *Bull. Nat. Inst. Sc. India* **38** 263

Sverdrup H U, Johnson M W and Fleming R H 1942 *The oceans* 500–501 (New Jersey: Prentice-Hall)

UNDP/FAO Pelagic Fishery Project (IND/93) Progress Report 3 1973 (Cochin: UNDP/FAO Pelagic Fishery Project)

UNDP/FAO Pelagic Fishery Project (IND/593) Progress Report 7 1974 (Cochin: UNDP/FAO Pelagic Fishery Project)

UNDP/FAO Pelagic Fishery Project (IND/593) Progress Report 16 1976 (Cochin: UNDP/FAO Pelagic Fishery Project)

US Navy Marine Climatic Atlas of the World Indian Ocean 1976 (Washington DC: US Government Printing Office) Vol. 3

Wyrtki K 1971 *Oceanographic atlas of the international Indian Ocean expedition* (Washington DC: US Government Printing Office)